ELSEVIER

Thermochimica Acta 339 (1999) 35–40

thermochimica acta

www.elsevier.com/locate/tca

Kinetic parameters of the thermal decomposition of trimethylindium by DSC

Thomas S. Fischer*, Norbert Eisenreich, Achim Pfeil

Fraunhofer Institut für Chemische Technologie, PO Box 1240, D-76327 Pfinztal, Germany

Received 11 August 1999; accepted 13 August 1999

Abstract

DSC curves of trimethylindium were recorded at different heating rates and crucible loading densities. The two dominating exothermic bands were kinetically analysed by fitting a two-step reaction model of first-order to the deconvoluted DSC data. The kinetic parameters, calculated at low loading densities, are $\log z_1 = 18.3 \pm 0.2\ s^{-1}$, $E_1 = 215.4 \pm 0.8$ kJ/mol and $\log z_2 = 9.3 \pm 0.2\ s^{-1}$, $E_2 = 139.2 \pm 0.8$ kJ/mol. © 1999 Elsevier Science B.V. All rights reserved.

Keywords: Reaction modelling; Kinetic analysis; Kinetic parameters; Thermal decomposition; DSC; Trimethylindium

1. Introduction

There are only a few DSC studies in the literature on the thermal decomposition of trimethylindium (TMI), most of them dealing with thermal stability, but none on kinetic parameters [1–3]. A kinetic analysis, however, is not straightforward. The TMI heat of decomposition is high, surpassing that of most conventional explosives. Low sample masses have to be used in the DSC experiment, combined with high-pressure crucibles of large thermal mass, causing a low sensitivity and a very slow thermal response of the measuring system. As a consequence, the thermal data have to be deconvoluted prior to analysis.

TMI is a commonly used precursor for organometallic vapour-phase epitaxy (OMVPE) of indium-containing films [4,5]. As with most metalorganic precursors, TMI is a difficult material to handle safely due to its thermal instability and its toxic and pyrophoric nature. On contact with air it can explode [6]. To ensure safe operating practices in production scale MOVPE or CBE (chemical beam epitaxy), kinetic decomposition parameters obtained at ambient and/or higher pressures are of particular importance. This work presents kinetic parameters of TMI by deconvoluting the DSC curves and fitting a specific reaction model to the deconvoluted data.

1.1. Kinetic reaction modelling

The modelling involves several steps:

- Construction of a baseline to correct for overlapping thermal events like evaporation.
- Deconvolution of the DSC signals to correct for the instrumental response.
- Assumption of a kinetic mechanism.
- Fitting of the assumed reaction model to the resulting curves using the kinetic parameters as fitting variables.

*Corresponding author. Fax: +49-721-4640111

0040-6031/99/$ – see front matter
PII: S0040-6031(99)00295-6

The response function for deconvolution was represented by two exponentials and was obtained from the endothermic melting peak of TMI in the DSC curve at the corresponding heating rate. The kinetic mechanism presented here assumes a two-step mechanism and simple first-order kinetics.

$$\frac{dy_1}{dt} = -k_1(T)y_1, \quad (1)$$

$$\frac{dy_2}{dt} = k_1(T)y_1 - k_2(T)y_2, \quad (2)$$

where $k_1(T) = z_1 \exp(-E_1/RT)$ and $k_2(T) = z_2 \exp(-E_2/RT)$. y_1 and y_2 denote the concentration of the reactants of step 1 and 2, respectively; k_1 and k_2 symbolize the corresponding reaction rate constants.

Eqs. (1) and (2) are solved for non-isothermal conditions on including the heating rate β.

$$y_1 = \exp(-S_1(T)), \quad (3)$$

$$y_2 = \exp(-S_2(T)) \int k_1(T) \exp(-S_1(T) \times \exp(S_2(T))\, dT), \quad (4)$$

where $S(T)$ denotes the following integral:

$$S(T) = z/\beta \int \exp(-E/RT)\, dT \cong T(RT/E - 2(RT/E)^2 + 6(RT/E)^3 - 24(RT/E)^4 + \cdots) \exp(-E/RT). \quad (5)$$

The fit curve $Q(T)$ is formed by

$$Q(T) = \sum Q_i dy_i/dt, \quad (6)$$

where Q_i denotes the heat of the respective reaction step.

2. Experimental

Owing to its toxic and pyrophoric nature, TMI sampling was carried out in an inert high-purity nitrogen atmosphere and the sample crucibles were hermetically sealed. High-pressure stainless steel crucibles were used with a design tolerance of 150 bar and they were gold plated for chemical inertness. The mass of the crucibles was 1.5 g and the volume 40 μl.

The DSC curves were recorded employing a Mettler Toledo heat-flux DSC 30 at heating rates of 2 and 5 K/min, covering the temperature range from 253 to 873 K. The sample masses ranged from 5.2 to 10.6 mg (LD 0.13–0.27 g/cm^3), thus varying the loading density (LD) by a factor of 2. The TMI used was manufactured by Epichem Ltd., England, and was high-purity electronic grade (99.9999% on the metal basis).

3. Results and discussion

Fig. 1 outlines the thermal events in the DSC curve at low LD in the temperature range 273–873 K. The exothermic decomposition is marked by two strong overlapping peaks at 558 K (exotherm I) and 630 K (exotherm II), measured at 5 K/min. A weak shoulder is noted in between at 570 K which becomes quite distinct when recorded at 2 K/min (cf. also [3]).

Table 1 lists the results of the best fits to the exotherms I and II after data deconvolution. Considering the experimental error, the kinetic parameters obtained at 2 and 5 K/min appear the same for the respective exotherm. However, on inspecting the correlation coefficients in Table 1, a significant difference is noted and the deviation becomes more obvious on consulting Figs. 2 and 3 which compare plots of the deconvoluted data to those of the best fit. Taking the difference curve as a measure, most disagreement occurs in Fig. 3 between 540 and 570 K at the position of the shoulder. On deconvolution, the descending slope of exotherm I looks steeper in Fig. 3 and the valley between the exotherms flatter than those in Fig. 2. Care was taken not to overshoot on deconvoluting

Table 1
Best fit kinetic parameters of the DSC exotherms I and II of TMI, recorded at high pressures in nitrogen

Heating rate (K/min)	LD (g/cm^3)	log z_1 (s^{-1})	E_1 (kJ/mol)	log z_2 (s^{-1})	E_2 (kJ/mol)	Correlation coefficient (%)
2	0.15	18.5 ± 0.4	214.7 ± 1.3	9.1 ± 0.3	139.0 ± 0.8	97.9
5	0.14	18.1 ± 0.4	216.0 ± 1.3	9.4 ± 0.3	139.4 ± 0.8	99.4

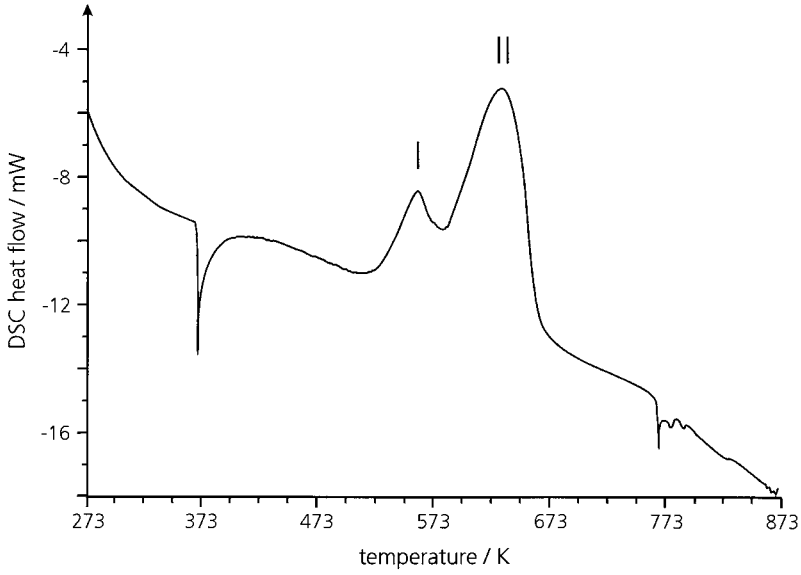

Fig. 1. DSC curve of TMI recorded at 5 K/min and 0.14 g/cm^3 loading density.

the experimental data and the structural changes could be the result of the Kissinger effect [7]. According to this effect, peaks belonging to different mechanistic events and having different kinetic parameters experience different temperature shifts on varying the heating rate. Hence, the unsteadiness in the difference curve between 540 and 570 K in Fig. 3 signals the presence of a further exotherm, buried beneath the slopes of exotherms I and II. The overlap, however, proved too close to apply a three-step model in the kinetic analysis and, because DSC records the overall effect, the parameters listed in Table 1 contain contributions of this non-resolved peak.

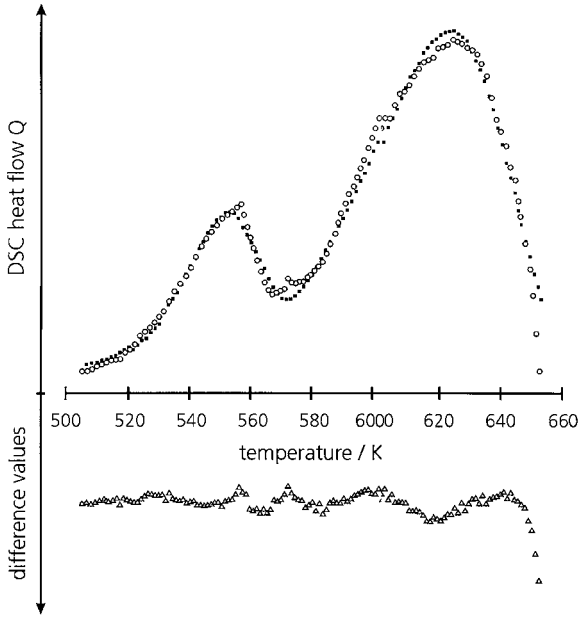

Fig. 2. Plots of the deconvoluted DSC curve (○), the best fit curve (■) of the two-step reaction model and the difference (Δ) of the two curves. Original DSC data recorded at 5 K/min and 0.14 g/cm^3 loading density.

Table 2 summarizes the kinetic parameters obtained from thermal decomposition studies on TMI in flow reactors [8–12]. Under flow conditions, the decomposition proceeds by sequential homolytic fission of the three In–C bonds. The observed activation energies thereby correspond directly to the bond dissociation energies and E_a in Table 2 was assigned to the energy for the cleavage of the first In–C bond and E_b to that of the third bond [13], involving the following mechanistic steps:

$$In(CH_3)_3 \rightarrow In(CH_3)_2 + CH_3 \quad (I)$$

$$In(CH_3) \rightarrow In_{metallic} + CH_3. \quad (II)$$

The cleavage of the second In–C bond could not be measured in the flow studies. It occurred rapidly and almost simultaneously with that of the first one

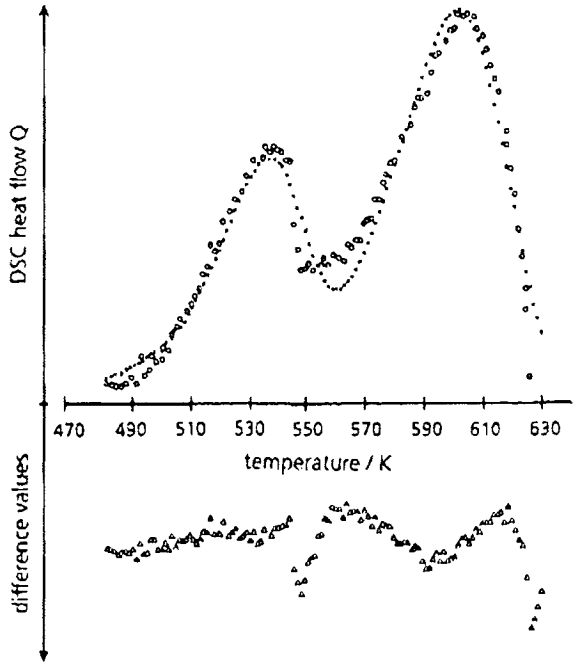

Fig. 3. Plots of the deconvoluted DSC curve (○), the best fit curve (■) of the two-step reaction model and the difference (Δ) of the two curves. Original DSC data recorded at 2 K/min and 0.15 g/cm^3 loading density.

[8,10,11] and estimations of the dissociation energy of this bond amount to 83.7 kJ/mol [13].

The kinetic parameters in Table 1 are in general agreement with those derived from the flow-studies, suggesting that the mechanism established at low pressures is also active in the DSC experiment. In the isobaric DTA decomposition of TMI at 1 bar, this mechanism was confirmed by GC product analysis [14], but in DSC isochoric conditions prevail.

The boiling point of TMI at 1 bar is 407 K [15] and the isochoric condition in the tightly sealed crucibles causes the pressure to rise as TMI melts, vaporizes and decomposes. The vaporization is not seen in the DSC curve but appears, for example, as an intense broad endotherm in the (isobaric) DTA curve of TMI at 1 bar [14]. At 673 K, the pressure buildup in the DSC crucible could amount to 78 bar, as was measured for the related trimethylaluminium at the same heating rate and LD in a special high-pressure cell [16,17]. Assuming a homolytic bond fission mechanism in the DSC experiment, a pressure of this magnitude is expected and, in view of the pressure, the rates must be higher with respect to those obtained from the flow studies, as expressed in the Tables 1 and 2.

Based on these findings, the exotherms I and II are assigned to the mechanistic steps (I) and (II); respectively. As judged from its position and intensity, the (non-resolved) peak positioned between the exotherms is attributed to the cleavage of the second In–C bond

$$\mathrm{In(CH_3)_2} \rightarrow \mathrm{In(CH_3) + CH_3}. \qquad \text{(III)}$$

Reaction (III) produces the intermediate monomethylindium (MMI) which, in turn, may further decompose to metallic indium as stated by reaction (II). The presence of metallic indium is manifested in the DSC curve by the characteristic melting endotherm on temperature cycling. As shown in flow reactors, MMI is quite stable and was identified in situ by its Raman spectrum [10,11]. In competition, MMI may also polymerize by forming a white precipitate on the reactor walls [8–11] and presumably is also produced in the DSC experiment, visible in Fig. 1 as the series of weak endotherms above 673 K. The latter are dependent on pressure and they increase in intensity with increasing LD. Fig. 4 shows such a curve recorded at 0.27 g/cm^3. The higher pressure causes the intensity of exotherm II to decrease with respect to that of exotherm I, favouring instead the formation of the MMI polymer, expressed in Fig. 4 by the strong increase in intensity of the melting endotherms above 673 K.

Table 2
Kinetic parameters of TMI pyrolysis in flow reactors at low partial pressures and in different atmospheres

Ambient	log z_a (s^{-1})	E_a (KJ/mol)	log z_b (s^{-1})	E_b (KJ/mol)	References
Toluene	15.7	197.6	10.9	162.0	[8]
Nitrogen	12.6	169.5	–	–	[9]
Hydrogen	12.0	150.3	–	–	[9]
Hydrogen	15.3	185.9	–	–	[12]

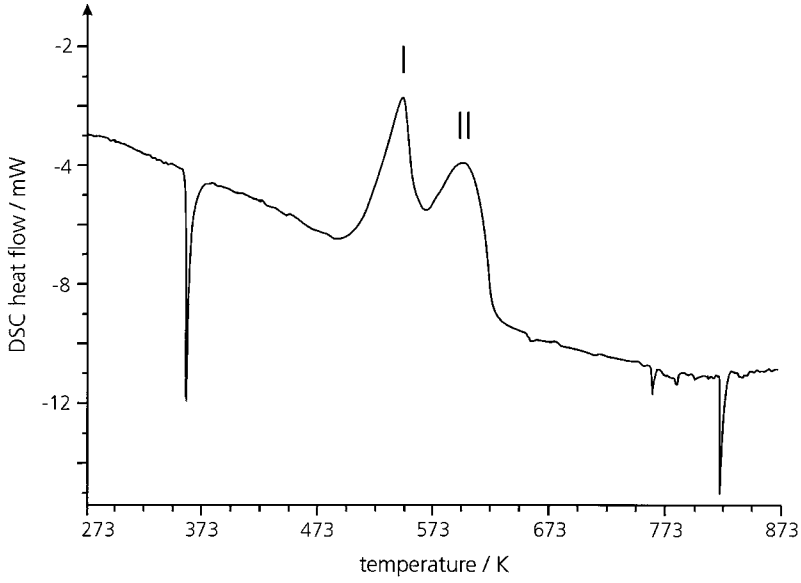

Fig. 4. DSC curve of TMI recorded at 2 K/min and 0.27 g/cm^3 loading density.

$$n\mathrm{In(CH_3)} \rightarrow [\mathrm{In(CH_3)}]_{n,\mathrm{polymeric}}. \quad \text{(IV)}$$

The intensity decrease of exotherm II in Fig. 4 leads to less overlap and causes the shoulder at 560 K to appear even more pronounced. Fig. 5 enlarges the pertinent part of the curve and its derivative clearly marks this (unresolved) peak as a significant exothermal event.

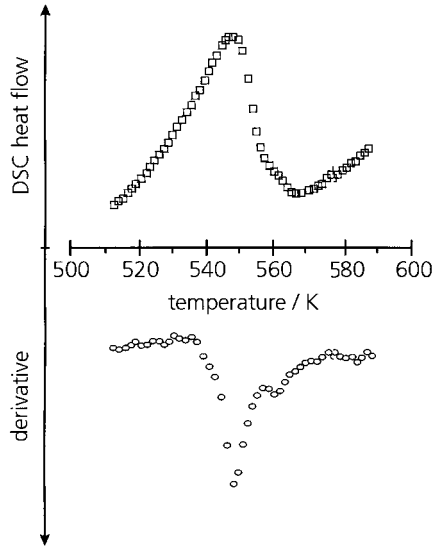

Fig. 5. Enlarged part of the DSC curve shown in Fig. 4 (□) and its derivative (○).

4. Conclusions

As observed in isobaric flow studies at low partial pressure, the isochoric decomposition of TMI by DSC proceeds by the sequential homolytic fission of the three In–C bonds, but only two strong exothermic bands are observed in the DSC curve. The fit of a two-step kinetic model to the deconvoluted exothermic data, recorded at low LD, resulted in kinetic parameters in general agreement with those derived from flow studies.

In the DSC curves, the ''missing'' peak is buried by the slopes of the strong exotherms, but is observed as a distinct shoulder at slow heating rates. The overlap, however, proved too close to allow fitting by a three-step kinetic model.

The decay of the intermediate monomethylindium to metallic indium competes with the formation of polymeric monomethylindium, the latter favoured at high loading densities. The polymer is stable up to 873 K and is observed in the DSC curves by its melting endotherms above 673 K.

Acknowledgements

The samples were provided by Epichem Ltd., Merseyside (UK). The work was financially supported in part by EU grant Contract No. EV5V-CT94-0414 and by DLR Projektträgerschaften Umwelttechnik, Förderkennzeichen 01 RG 9520/5.

References

[1] X. Li, D.F. Foster, D.J. Cole-Hamilton, Polym. Adv. Technol. 5 (1994) 541.
[2] T.S. Fischer, A. Pfeil, N. Eisenreich, A.C. Jones, A.B. Leese, S. Rushworth, G. Williams, Proceedings of the 26th International Annual Conference of ICT, 1995, pp. 85/1–85/6.
[3] S. Duffy, P.F. Nolan, S. Rushworth, A.B. Leese, A.C. Jones, Adv. Mater. Opt. Electron 7 (1997) 233.
[4] A.C. Jones, A.K. Holiday, D.J. Cole-Hamilton, J. Cryst. Growth 68 (1984) 1.
[5] A.C. Jones, J. Crystal Growth 129 (1993) 728.
[6] R.M. Content, Control methods for metals and metalloids in III–V materials vapour-phase epitaxy, in: Hazard Assessment and Control Technology in Semiconductor Manufacturing, Industrial Hygiene Science Series, Chelsea, Michigan, 1989.
[7] H.E. Kissinger, Anal. Chem. 29 (1957) 1702.
[8] M.G. Jacko, S.J.W. Price, Can. J. Chem. 42 (1964) 1198.
[9] C.A. Larsen, G.B. Stringfellow, J. Crystal Growth 75 (1986) 247.
[10] Z.S. Huang, Proc. Electrochem. Soc. 93 (1993) 2.
[11] Z.S. Huang, Chino Park, T.J. Anderson, Proceedings of the12th International Symposium on Vapor Deposition, 1993, pp. 13–19.
[12] M. Sugiyama, K. Kusunoki, Y. Shimogaki, S. Sudo, Y. Nakano, H. Nagamoto, K. Sugawara, K. Tada, H. Komiyama, Appl. Surf. Sci. 116/117 (1997) 746.
[13] S.J.W. Price, in: C.H. Bramford, C.F.H. Tipper (Eds.), Comprehensive Chemical Kinetics, vol. 4, chap. 4, Elsevier, Amsterdam, 1972, pp. 253.
[14] N.N. Travkin, P.K. Skachkov, I.G. Tonoyan, B.I. Kozyrkin, J. Gen. Chem. USSR 48 (1978) 2428 (Engl. Transl.).
[15] Product Information and Materials Safety Data Sheet, Epichem Limited, Merseyside, UK.
[16] Accident Prevention of Metalorganic Precursors (APMOP), Summary Report, contract EV5V-CT94-0414, 1996
[17] Unfallverhütung bei der Handhabung metallorganischer Verbindungen, Schlußbericht, Förderkennzeichen 01 RG 9520/5, DLR Projektträgerschaft Umwelttechnik, 1996.